

Characterisation and investigation of antibacterial properties of nylon 66/TPS/Ag NPs nanofibre membranes

Alireza Allafchian¹ ✉, Seyed Amir Hossein Jalali^{2,3}, Navida Kabirzadeh³

¹Research Institute for Nanotechnology and Advanced Materials, Isfahan University of Technology, Isfahan 84156-83111, Iran

²Department of Natural Resources, Isfahan University of Technology, Isfahan 84156-83111, Iran

³Research Institute for Biotechnology and Bioengineering, Isfahan University of Technology, Isfahan 84156-83111, Iran

✉ E-mail: allafchian@cc.iut.ac.ir

Published in *Micro & Nano Letters*; Received on 7th May 2018; Revised on 12th August 2018; Accepted on 10th September 2018

Electrospinning method was used to prepare nylon 66 nanofibre membranes in solution mixed with chloroform/formic acid. These nanofibres were covered with (3-mercaptopropyl) trimethoxysilane (TPS) that has a sulphur group, making it a suitable host for Ag nanoparticles (Ag NPs). Spraying of the as-prepared nylon 66/TPS surface first with silver nitrate solution and then scattering with a mixture of $N_2H_4/NaBH_4$ used as reducing agents during the second process provides nanofibres with nylon 66/TPS/Ag NPs structure. Characterisation of the formed nanofibres was studied by Fourier transform infrared, scanning electron microscopy, X-ray diffraction and transmission electron microscopy techniques. The non-woven polyurethane coated with activated carbon particles and polyethylene mesh was utilised as the substrate and protective layers of as-prepared nanofibres, respectively. Finally, the antibacterial activity of nanofibre membranes against gram-positive and gram-negative bacteria was investigated by using the disk diffusion method and it was shown that the newly synthesised nanofibres presented very good antibacterial activity against the tested bacteria. The results of this study can be used for industrial applications such as antibacterial wound dressings or/and water disinfection filters.

1. Introduction: The industrial applications of Ag nanoparticles (Ag NPs) such as in medicine, catalysis, solar energy, lithography and photocatalysis and especially their antibacterial activities against some microorganisms have been proved [1–6]. When using Ag NPs, toxic Ag ions are formed in media and this has limited their applications. The immobilisation of Ag NPs on the supporting agents has solved this problem to a certain extent. The general supporting agents used are polymers [7, 8], chitosan [9], zeolite [10] and particularly nanoferrites [11].

Using nanoferrite materials has some advantages such as convenient immobilisation of Ag NPs and their separation from media by the application an external magnetic field after disinfection process [8, 12]. However, application of magnetic field with very high potential is not applicable at an industrial scale, for example, in water treatment of rivers and in some cases like treatment of bactericidal wounds. In these cases, the nanofibres can be a suitable replacement of nanoferrites and untangled moot point.

The technological applications of polymers have become advanced in many areas of nanotechnology due to their physical and chemical properties [13]. The main components of the constituent single-layer nanofibres are polymers based on which they are named as poly(vinylidene fluoride) [14], polytetrafluoroethylene [15], polyacrylonitrile (PAN) [16], poly(methyl methacrylate) [17], poly(vinyl alcohol) [18], polyurethane [19], carbon nanofibre [20], cellulose acetate [21], polyamide [22], nylon 6 [23] and nylon 66 [24]. Also, some hybrid nanofibres with a wide range of industrial and medical applications such as in sensors, fuel cell, catalysis and biomedical materials are more functional than single-layer nanofibres and here too, polymers are one of the chief components. poly(tetrafluoroethylene)/ poly(amide) [25], polydopamine/graphene oxide [26], poly(vinyl alcohol)/montmorillonite [27], polylactide poly(lactic acid) [28], β -cyclodextrin/PAN [29], TiO_2 /nylon 6 [30] and chitosan/poly(vinyl alcohol) [31] as supporting agents of Ag NPs were successfully used. In particular, polymer nanofibres having large surface area and different surface functionalities for their utilization in various applications, such as engineering of tissue, drug delivery and antibacterial activities in wounds, are of interest [32].

One of the most significant commercial fibres produced is nylon that can be converted to nanofibres. Nylon 66 is one of the greatest and most important types of nylon which is prepared by the process of polycondensation. In this research, nylon 66 was prepared by electrospinning process. Then, (3-mercaptopropyl) trimethoxysilane (TPS) material was loaded on the surface of nanofibres nylon 66, and nylon 66/TPS was prepared. At the end, Ag NPs were immobilised on nylon 66/TPS surface and nylon 66/TPS/Ag NPs fibres were synthesised. The characterisation was investigated by using Fourier transform infrared (FTIR), transmission electron microscopy (TEM) and field emission scanning electron microscopy (FE-SEM) techniques. After confirmation of the mentioned nanofibres fabrication, their antibacterial activities against two gram-negative and gram-positive bacteria were studied by disk diffusion method. The observation of brilliant antimicrobial activity indicates that this newly synthesised nanofibres membrane can be used as filter for treating polluted water as well as in wound healing.

2. Experimental

2.1. Materials and methods: The polymerised nylon 66 (SSP PA66) with the molecular weight of 50,625 g/mol was bought from Zanjan Tire Cord, Iran. The chloroform and formic acid were prepared from Merck (Germany) as the solvents of nylon 66. The density and boiling point of the chloroform and formic acid were 1.47 and 1.22 g/ml and 61 and 101°C, respectively. Also, TPS, HCl, ethanol, $AgNO_3$ and $NaBH_4$ were obtained from Merck (Germany). All solutions were prepared in double distilled water.

The electrospinning system was constructed at Fanavaran Nano Meghyas Co. (Iran). This instrument consisted of a high voltage supply (Emersun, 220 V, AC input – up to 35 kV DC output), a dosing pump (MEDIFusion MS-2200, Korea) with feeding capacity of 10–100 ml/h, syringe (1 ml) connected to a blunt tipped needle (internal diameter=0.5 mm) connected to the positive electrode and aluminium foil as collector which was connected to the positive and negative electrodes.

The FTIR spectrum was gained by applying a FTIR Jasco Japan spectrophotometer. The FE-SEM images of the nanofibres were achieved by Hitachi Japan S4160 scanning electron microscope.

The morphology and size of the as-synthesised nanoparticles were determined by applying a Philips CM10-HT 100KV microscope from the Netherland for gaining TEM images. X-ray powder diffraction (Philips EXPERT) using a Cu-K α radiation source in the range of 10–80 $^\circ$, for 2θ was used as an analytical technique for phase identification of magnetic core-shell nanoparticle.

2.2. Construction of nylon 66 nanofibre membranes: To prepare nanofibre membranes from polymer solution, concentration is an important parameter. Due to the restricted concentration, the optimal conditions that are obtained in the previous work were used [33]. Therefore, the electrospinning polymer solution concentration was 23% (w/w) and in the mixed solution of formic acid/chloroform it was 3% (v/v). This solution was stirred for 24 h to obtain a homogenous solution. The physical and electronic properties that are used for electrospinning are as follows: the utilised voltage was adjusted 12.5 kV (Emerson, China) between the nozzle and collector that were at a distance of \sim 15 cm. The inner diameter of needle syringe was 0.5 mm. The solution flow rate was set at 0.314 ml/h (Terumo, Japan) and the traversed speed of syringe pump was 4 cm/min. The nanofibre composites were gathered on an aluminium foil. The polyurethane mesh was applied as the substrate. The fibre electrospinning was done at room temperature under atmospheric conditions.

2.3. Preparation of modified nanofibre membranes: After producing nylon 66 nanofibre membranes, TPS solution, water, ethanol and HCl in the molar ratio of 4:200:50:0.1 was mixed. In this mixture, 2.5 ml TPS, 8.12 ml water, 5.2 ml ethanol and 15 μ l HCl 37% were sprayed onto the surface of the membranes and maintained in the ambient temperature for 1 day. The nylon 66 nanofibre membrane surface was functionalised by this method and nylon 66/TPS membrane was prepared.

2.4. Producing nylon 66/TPS/Ag NPs membranes: First, the as-prepared nylon 66/TPS nanofibre was sprayed with 0.1 M silver nitrate solution and during the second process, a mixture of 0.1 M N $_2$ H $_4$ /NaBH $_4$ that were used as reducing agents was scattered on the nylon 66/TPS/Ag+ surface to produce nanofibre with nylon 66/TPS/Ag NPs structure. After 2 min, the surface of the newly formed nanofibre was washed at room temperature three times with distilled water for removing the excess Ag NO $_3$ that was formed. Then, the polyethylene mesh was utilised as a protective layer of prepared nylon 66/TPS/Ag NPs membranes.

2.5. Antibacterial activity, minimum inhibitory concentration (MIC) and minimum bactericidal concentration (MBC) investigation: The microbicidal properties of the synthesised nanofibres was studied by using the Kirby–Bauer disk diffusion procedure. Also, the MIC and MBC were measured and studied. In summary, the *Escherichia coli* and *Salmonella typhimurium* as gram negative bacteria, and *Staphylococcus aureus* and *Bacillus cereus* as gram positive bacteria were selected for the evaluation of the antibacterial potency. The turbidity of bacterial suspensions was adjusted at the 0.5 McFarland standard. The standard antibiotic disk of the Ag NPs and synthesised nanofibres nylon 66/TPS and nylon 66/TPS/Ag NPs with 1×1 cm 2 dimensions were prepared, and distilled water was applied as a negative control. Four Mueller–Hinton agar plates (Merck, Germany) containing cultures of various bacterial strains were applied to evaluate the antibacterial activity. Impregnated disks and as-synthesised square nanofibres were located on the surface of the agar and incubated at 37 $^\circ$ C for 24 h to control the antimicrobial activity.

For the MIC test study, the process of sample dilution process was done after the electrospinning nanofibres of nylon 66/TPS. About 30 μ l AgNO $_3$ solutions with 6.25, 12.5, 25, 50 and

100 ppm concentrations was sprayed on the nanofibre surface with 0.5×0.5 cm 2 dimensions, separately. Then, reducing agent was added to Ag NPs formation on the nylon 66/TPS surface. The tubes contain 1 ml of the 10 6 CFU bacteria solutions and incubated at 37 $^\circ$ C for 24 h. The MIC was documented for the maximum diluted solution without the growth of bacteria. Then, the tubes which no growth were located onto nutrient agar and incubated at 37 $^\circ$ C for 24 h for the MBC determination. The highest dilutions tube without clear growth was considered as the MBC value.

3. Results and discussion

3.1. Scanning electron microscopy (SEM) results: The SEM images of as-synthesised nanofibre membranes nylon 66/TPS and nylon 66/TPS/Ag NPs were taken and are shown in Fig. 1. The Digimizer software was used for nanofibres diameter determination. The results for ten measurements were listed in Table 1. It is obvious that with increasing of Ag NPs layer on nylon 66/TPS, the mean diameter of nanofibre increases. This increment has been obtained as 44.0 ± 4.5 nm.

3.2. TEM results: The TEM image of the nylon 66/TPS/Ag NPs nanofibres membrane was investigated and shown in Fig. 2. The formation of spherical Ag NPs on the nanofibre membrane is clearly observable. The size distribution of the Ag NPs on the surface of nanofibre membrane is averaged as 39 nm.

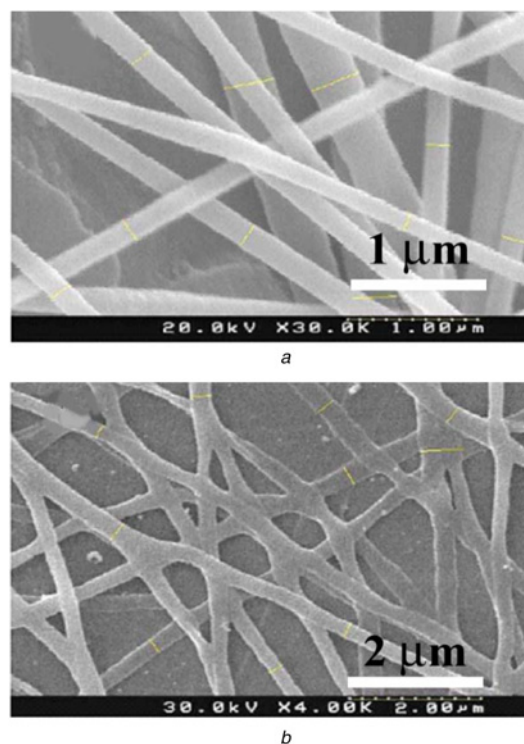


Fig. 1 SEM images of
a Nylon 66/TPS
b Nylon 66/TPS/Ag NPs

Table 1 Diameter (nm) of nylon 66/TPS and nylon 66/TPS/Ag NPs nanofibres membrane

Nanofibres membrane	<i>n</i>	Min	Max	Mean
nylon 66/TPS	10	155 \pm 1	406 \pm 1	232 \pm 1
nylon 66/TPS/Ag NPs	10	221 \pm 8.6	368 \pm 8.6	276 \pm 9

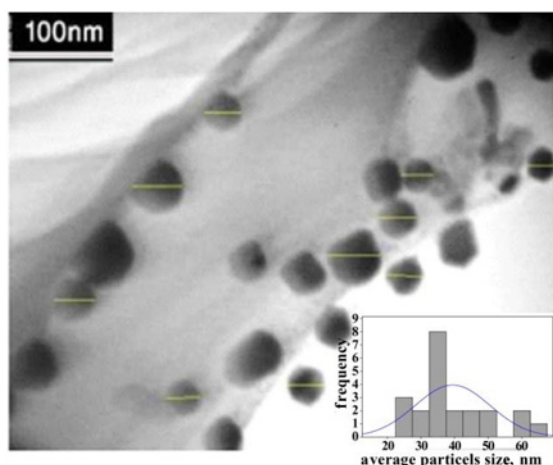


Fig. 2 TEM images of nylon 66/TPS/Ag NPs

3.3. FTIR studies: The FTIR spectra of nylon 66 and nylon 66/TPS were scanned and assigned in Fig. 3. The C–C stretching of nylon 66 was observed at around 935.5 cm^{-1} . The peaks at around 1542 and 1642.3 cm^{-1} were attributed to amide II and amide I bonds, respectively. The C=O and N–H stretchings were assigned at around 1733.5 and 3302.2 cm^{-1} , respectively. The peaks at around 2928.5 , 2861 and 3081 cm^{-1} were attributed to C–H₂ and C–H asymmetric stretchings and individually [34]. The chemical bonding between Si atom of TPS and amine group of nylon 66 was presented in Fig. 4.

After that the TPS was covered by nylon 66 surface, the FTIR spectra has not been significantly changed except regions between 800 and 1300 cm^{-1} . The bond at around 2559.8 cm^{-1} is assigned to S–H stretching. The Si–O–C stretching symmetry was assigned at around 820 cm^{-1} . The C–C bond was observed at 1047.5 cm^{-1} . The symmetrical stretching and torsion of CH₂ bonds were observed at around 2866.5 and 1112.6 and 1251 cm^{-1} , respectively [35]. The reduced intensity of the peaks at 1500 – 2000 indicates that TPS interact with nylon 66 and nylon 66/TPA has been formed.

3.4. X-ray diffraction (XRD) analysis: The XRD patterns of as-synthesised nanofibre membranes nylon 66/TPS/Ag NPs are

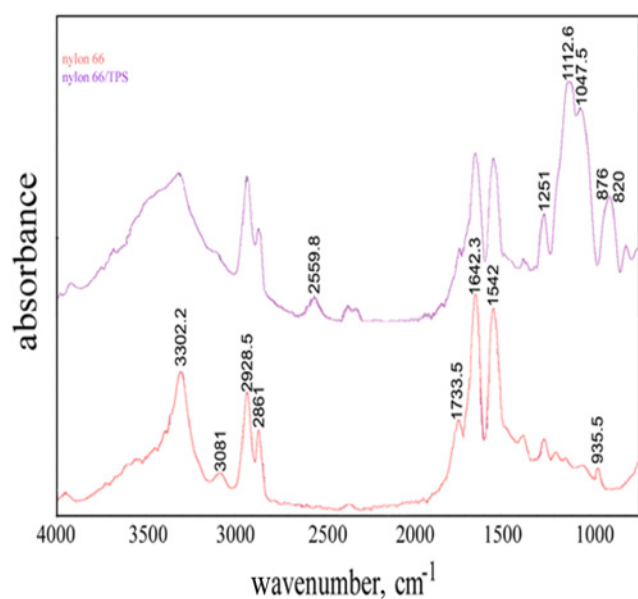


Fig. 3 FTIR spectra assignment of nylon 66 and nylon 66/TPS

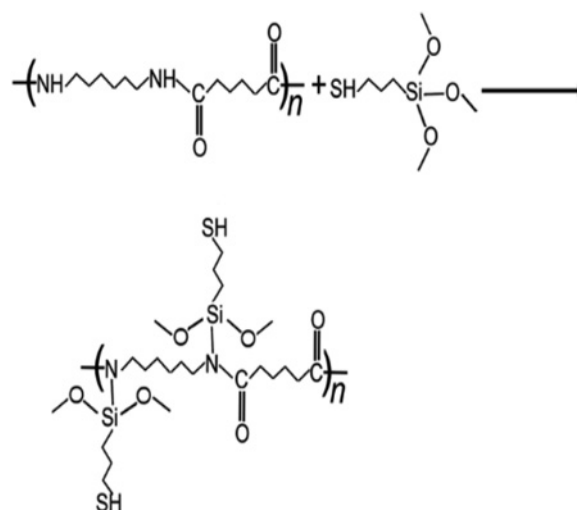


Fig. 4 Chemical bonding between TPS and amine nylon 66

shown in Fig. 5. As shown in the diagram, the peak characteristic of Ag NPs was located in the range of 38.1° , 44.3° , 64.5° and 77.7° . The values of the (hkl) for these angles were (111), (200), (220) and (311), respectively. Following that, it turned out that the Ag NPs possessed a cubic structure along with a full sides centre. Also, the position of the mentioned peaks was matched with JCPDS Card No. 04-0783. The average crystal size of Ag NPs is estimated around 42 nm by using Scherrer equation. Two strong diffraction peaks at $2\theta \approx 20.4^\circ$ and 24.1° were observed in Fig. 5, showing, via the star sign, that the mentioned peaks were related to the α phase of nylon 66, which are designated as α_1 and α_2 , respectively [36].

3.5. Results of antibacterial activity: The disk diffusion method was applied to analyse the antibacterial activities of nylon 66/TPS, nylon 66/TPS/Ag NPs and Ag NPs; and distilled water was applied as a negative control. Two different gram-positive (*S. aureus* and *B. cereus*) and gram-negative (*E. coli* and *S. typhimurium*) bacteria were studied and corresponding to Fig. 6, the diameters of growth inhibition are measured as criteria of microbicidal activity. The presented results in Table 2 show that only Ag NPs and nanofibre membrane have antibacterial properties. The most surprising result of microbicidal activity relates to nylon 66/TPS/Ag NPs nanofibre membrane and indicates that this newly synthesised nanofibre can be used in water treatment as a filter or wound healing. Although further study is required to have a clear understanding of the mechanism of silver nanoparticles against different bacteria [37], it is

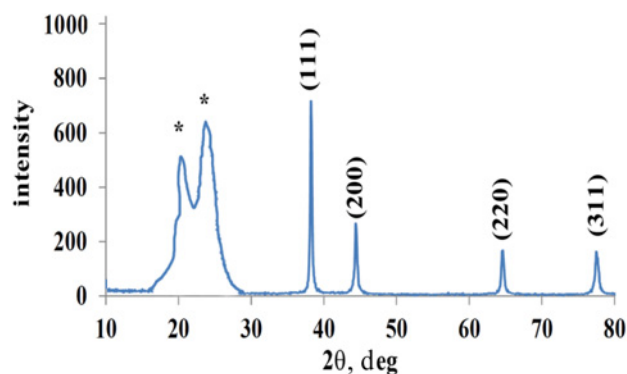


Fig. 5 XRD patterns of nylon 66/TPS/Ag NPs

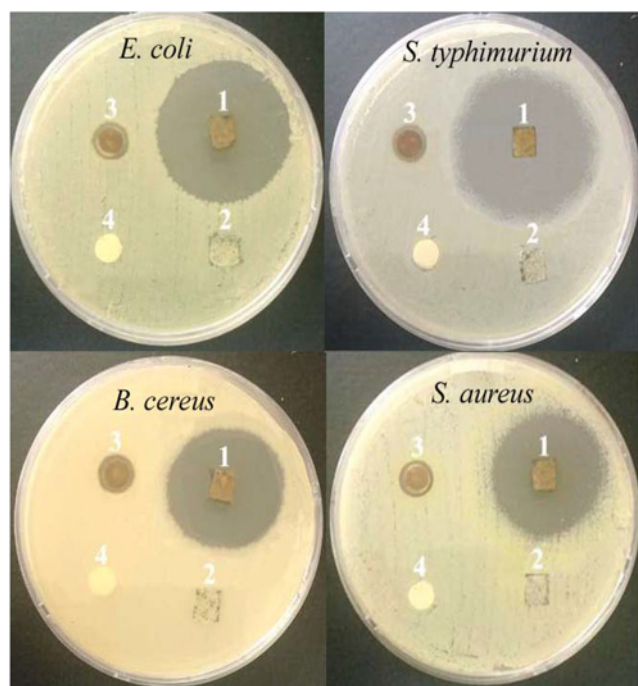


Fig. 6 Inhibition zone of 1: nylon 66/TPS/Ag NPs, 2: nylon 66/TPS, 3: Ag NPs and 4: distilled water against tested various bacteria

Table 2 Zone inhibition of the Ag NPs, nylon 66/TPS, nylon 66/TPS/Ag NPs and distilled water against tested bacteria

Bacteria	Zone of inhibition (mm) average \pm standard deviation			
	Distilled water	Ag NPs	Nylon 66/TPS	Nylon 66/TPS/Ag NPs
<i>E. coli</i>	6.4 \pm 0.1	8.4 \pm 0.1	N.D	31.2 \pm 0.2
<i>S. typhimurium</i>	6.4 \pm 0.1	8.1 \pm 0.1	N.D	31.7 \pm 0.2
<i>S. aureus</i>	6.4 \pm 0.1	8.5 \pm 0.1	N.D	27.5 \pm 0.2
<i>B. cereus</i>	6.4 \pm 0.1	8.7 \pm 0.1	N.D	27.6 \pm 0.2

Table 3 MIC (μ g/ml) and MBC (μ g/ml) of the as-prepared the nylon 66/TPS/Ag NPs nanofibre and Ag NPs

Bacteria	Nylon 66/TPS/Ag NPs		Ag NPs		(MBC/MIC) _{nanofibre} / (MBC/MIC) _{Ag NPs}
	MIC	MBC	MIC	MBC	
<i>S. aureus</i>	12.5	25	25	50	2 / 2
<i>B. cereus</i>	12.5	25	25	50	2 / 2
<i>E. coli</i>	6.25	12.5	12.5	25	2 / 2
<i>S. typhimurium</i>	6.25	12.5	12.5	25	2 / 2

suggested that Ag NPs get attached to the surface (cell membrane) of the bacteria which interrupts in main functions such as permeability and respiration of the bacteria. Hence, the binding of nanoparticles to the bacteria relies evidently on the available surface area for interaction [38].

The MIC and MBC values of Ag NPs and nylon 66/TPS/Ag NPs nanofibre against gram-negative and gram-positive bacteria are listed in Table 3. The MBCs range changes of nylon 66/TPS/Ag NPs nanofibre and Ag NPs are from 12.5 to 25.0 and 25 to

50 mg/ml, respectively, that shows the bactericidal activity of nanofibre is very higher than Ag NPs. The ratio of MBC/MIC is ≤ 4 and equal to 2 for nanofibre and Ag NPs that indicates that a strong antibacterial activity against the tested bacterial strains is for Ag NPs and nylon 66/TPS/Ag NPs nanofibre.

4 Conclusion: The nylon 66/TPS/Ag NPs nanofibre was prepared by using electrospinning procedure. After characterisation using SEM, TEM and FTIR techniques, the antibacterial activity of the as-synthesised nanofibre membranes against gram-positive and gram-negative bacteria was investigated by using the disk diffusion method. The average width of the nylon 66/TPS and nylon 66/TPS/Ag NPs nanofibres were estimated to be 0.250 and 0.325 μ m from the SEM study. The TEM result showed that the spherical Ag NPs localised on the surface of nylon 66/TPS, and their size distribution is estimated to be 37.9 nm. The zone inhibition of antibacterial activity consequences was obtained 31.2, 31.7, 27.5 and 27.6 mm against *E. Coli*, *S. typhimurium*, *S. aureus* and *B. cereus*, respectively. Therefore this nanofibre can be used in industry and medical applications such as in filtration systems and wound healing.

5 References

- [1] Prabhu S., Poulse E.K.: 'Silver nanoparticles: mechanism of antimicrobial action, synthesis, medical applications, and toxicity effects', *Int. Nano. Lett.*, 2012, **2**, (1), pp. 1–10
- [2] Pradhan N., Pal A., Pal T.: 'Silver nanoparticle catalyzed reduction of aromatic nitro compounds', *Colloids Surf., A*, 2002, **196**, (2–3), pp. 247–257
- [3] Chen X., Jia B., Saha J.K., *ET AL.*: 'Broadband enhancement in thin-film amorphous silicon solar cells enabled by nucleated silver nanoparticles', *Nano Lett.*, 2012, **12**, (5), pp. 2187–2192
- [4] Sherly Arputha Kiruba V., Dakshinamurthy A., Subramanian P.S., *ET AL.*: 'Green synthesis of biocidal silver-activated charcoal nanocomposite for disinfecting water', *J. Exp. Nanosci.*, 2015, **10**, (7), pp. 532–544
- [5] Mariselvam R., Ranjitsingh A.J.A., Usha Raja Nanthini A., *ET AL.*: 'Green synthesis of silver nanoparticles from the extract of the inflorescence of *Cocos nucifera* (family: Arecaceae) for enhanced antibacterial activity', *Spectrochim. Acta A*, 2014, **129**, (14), pp. 537–541
- [6] Allafchian A.R., Mirahmadi-Zare S.Z., Jalali S.A.H., *ET AL.*: 'Green synthesis of silver nanoparticles using phlomis leaf extract and investigation of their antibacterial activity', *J. Nanostruct. Chem.*, 2016, **6**, (2), pp. 129–135
- [7] Horváth B., Kawakita J., Chikyow T.: 'Adhesion of silver/ polypyrrole nanocomposite coating to a fluoropolymer substrate', *Appl. Surf. Sci.*, 2016, **384**, pp. 492–496
- [8] Allafchian A.R., Jalali S.A.H., Amiri R., *ET AL.*: 'Synthesis and characterization of the NiFe₂O₄@TEOS-TPS@Ag nanocomposite and investigation of its antibacterial activity', *Appl. Surf. Sci.*, 2016, **385**, pp. 506–514
- [9] Mironenko A., Modin E., Sergeev A., *ET AL.*: 'Fabrication and optical properties of chitosan/Ag nanoparticles thin film composites', *Chem. Eng. J.*, 2014, **244**, pp. 457–463
- [10] Inoue Y., Hoshino M., Takahashi H., *ET AL.*: 'Bactericidal activity of Ag–zeolite mediated by reactive oxygen species under aerated conditions', *J. Inorg. Biochem.*, 2002, **92**, (1), pp. 37–42
- [11] Tang D., Yuan R., Chai Y.: 'Magnetic core-shell Fe₃O₄@Ag nanoparticles coated carbon paste interface for studies of carcinoembryonic antigen in clinical immunoassay', *J. Phys. Chem. B*, 2006, **110**, (24), pp. 11640–11646
- [12] Allafchian A., Bahramian H., Jalali S.A.H., *ET AL.*: 'Synthesis, characterization and antibacterial effect of new magnetically core-shell nanocomposites', *J. Magn. Magn. Mater.*, 2015, **394**, pp. 318–324
- [13] Bicerano J.: 'Prediction of polymer properties' (Marcel Dekker, New York, NY, 2002)
- [14] Sheikh F.A., Zargar M.A., Tamboli A.H., *ET AL.*: 'A super hydrophilic modification of poly(vinylidene fluoride) (PVDF) nanofibers: By in situ hydrothermal approach', *Appl. Surf. Sci.*, 2016, **385**, pp. 417–425
- [15] Guo R., Yin G., Sha X., *ET AL.*: 'The significant adhesion enhancement of Ag–polytetrafluoroethylene antibacterial coatings by using of molecular bridge', *Appl. Surf. Sci.*, 2015, **341**, pp. 13–18

- [16] Mahapatra A., Garg N., Nayak B., *ET AL.*: 'Studies on the synthesis of electrospun PAN-Ag composite nanofibers for antibacterial application', *Appl. Surf. Sci.*, 2012, **124**, (2), pp. 1178–1185
- [17] Kong H., Jang J.: 'Antibacterial properties of novel poly (methyl methacrylate) nanofiber containing silver nanoparticles', *Langmuir*, 2008, **24**, (5), pp. 2051–2056
- [18] Hong K.H., Park J.L., Sul I.H., *ET AL.*: 'Preparation of antimicrobial poly (vinyl alcohol) nanofibers containing silver nanoparticles', *J. Polym. Sci., Part B: Polym. Phys.*, 2006, **44**, (17), pp. 2468–2474
- [19] Amarjargal A., Tijing L.D., Shon H.K., *ET AL.*: 'Facile in situ growth of highly monodispersed Ag nanoparticles on electrospun PU nanofiber membranes: flexible and high efficiency substrates for surface enhanced Raman scattering', *Appl. Surf. Sci.*, 2014, **308**, pp. 396–401
- [20] Singh S., Ashfaq M., Singh R.K., *ET AL.*: 'Preparation of surfactant-mediated silver and copper nanoparticles dispersed in hierarchical carbon micro-nanofibers for antibacterial applications', *New biotechnol.*, 2013, **30**, (6), pp. 656–665
- [21] Wang K., Qian M., Wang S.D., *ET AL.*: 'Electrospinning of silver nanoparticles loaded highly porous cellulose acetate nanofibrous membrane for treatment of dye wastewater', *Appl. Phys. A.*, 2016, **122**, (1), pp. 1–10
- [22] Hee P.S., Seon K.Y., Joon P.S., *ET AL.*: 'Immobilization of silver nanoparticle-decorated silica particles on polyamide thin film composite membranes for antibacterial properties', *J. Membr. Sci.*, 2016, **499**, pp. 80–91
- [23] Bishweshwar P., Raj P.H., Raj P.D., *ET AL.*: 'Characterization and antibacterial properties of Ag NPs loaded nylon-6 nanocomposite prepared by one-step electrospinning process', *Colloids Surf., A*, 2012, **395**, pp. 94–99
- [24] Sedaghat S., Nasseri A.: 'Synthesis and stabilization of Ag nanoparticles on a polyamide (nylon 6, 6) surface and its antibacterial effects', *Int. Nano Lett.*, 2011, **1**, (1), p. 22
- [25] Carvalho D., Sousa T., Morais P.V., *ET AL.*: 'Polymer/ metal nanocomposite coating with antimicrobial activity against hospital isolated pathogen', *Appl. Surf. Sci.*, 2016, **379**, pp. 489–496
- [26] Zhou H., Liu Y., Chi W., *ET AL.*: 'Preparation and antibacterial properties of Ag@polydopamine/graphene oxide sheet nanocomposite', *Appl. Surf. Sci.*, 2013, **282**, pp. 181–185
- [27] Hyeung P.J., Rezaul K.M., Kyo K.I., *ET AL.*: 'Electrospinning fabrication and characterization of poly(vinyl alcohol)/montmorillonite/silver hybrid nanofibers for antibacterial applications', *Colloid. Polym. Sci.*, 2009, **288**, (1), pp. 115–121
- [28] Sun Z., Fan C., Tang X., *ET AL.*: 'Characterization and antibacterial properties of porous fibers containing silver ions', *Appl. Surf. Sci.*, 2016, **387**, pp. 828–838
- [29] Wang S., Bai J., Li C., *ET AL.*: 'Functionalization of electrospun β -cyclodextrin/polyacrylonitrile (PAN) with silver nanoparticles: broad-spectrum antibacterial property', *Appl. Surf. Sci.*, 2012, **261**, pp. 499–503
- [30] Pant H.R., Pandeya D.R., Nam K.T., *ET AL.*: 'Photocatalytic and antibacterial properties of a TiO₂/nylon-6 electrospun nanocomposite mat containing silver nanoparticles', *J. Hazard. Mater.*, 2011, **189**, (1), pp. 465–471
- [31] Son B., Yeom B.Y., Song S.H., *ET AL.*: 'Antibacterial electrospun chitosan/poly (vinyl alcohol) nanofibers containing silver nitrate and titanium dioxide', *J. Appl. Polym. Sci.*, 2009, **111**, (6), pp. 2892–2899
- [32] Katti D.S., Robinson K.W., Ko F.K., *ET AL.*: 'Bioresorbable nanofiber-based systems for wound healing and drug delivery: optimization of fabrication parameters', *J. Biomed. Mater. Res. B, Appl. Biomater.*, 2004, **70**, (2), pp. 286–296
- [33] Shahram Forouz F., Ravandi S.A.H., Allafchian A.R.: 'Removal of Ag and Cr heavy metals using nanofiber membranes functionalized with aminopropyltriethoxysilane (APTES)', *Curr. Nano Sci.*, 2016, **12**, pp. 266–274
- [34] Charles J., Ramkumaar G.R., Azhagiri S., *ET AL.*: 'FTIR and thermal studies on nylon-66 and 30% glass fibre reinforced nylon-66', *J. Chem.*, 2009, **6**, (1), pp. 23–33
- [35] Thompson W.R., Mei Cai M.H., Pemberton J.E.: 'Hydrolysis and condensation of self-assembled monolayers of (3-mercaptopropyl) trimethoxysilane on Ag and Au surfaces', *Langmuir*, 1997, **13**, pp. 2291–2302
- [36] Mehrabian M., Nasr-Esfahani M.: 'HA/nylon 6,6 porous scaffolds fabricated by salt-leaching/solvent casting technique: effect of nano-sized filler content on scaffold properties', *Int. J. Nanomed.*, 2011, **6**, pp. 1651–1659
- [37] Allafchian A.R., Farhang H., Jalali S.A.H., *ET AL.*: 'Gundelia tournefortii L.: a natural source for the green synthesis of silver nanoparticles', *IET Nanobiotechnol.*, 2017, **11**, (7), pp. 815–820
- [38] Ahmed M.J., Murtaza G., Mehmood A., *ET AL.*: 'Green synthesis of silver nanoparticles using leaves extract of *Skimmia laureola*: characterization and antibacterial activity', *Mater. Lett.*, 2015, **153**, pp. 10–13